Fragile ground state and rigid field-induced structures in the zigzag ladder compound BaDy$_2$O$_4$

D. D. Khalyavin,[1] P. Manuel,[1] M. Ciomaga Hatnean [ORCID],[2] and O. A. Petrenko[2]

[1]*ISIS Facility, STFC Rutherford Appleton Laboratory, Chilton, Didcot, OX11 0QX, United Kingdom*
[2]*Department of Physics, University of Warwick, Coventry CV4 7AL, United Kingdom*

We report on a sequence of field-induced transitions in the zigzag ladder compound BaDy$_2$O$_4$ studied with powder neutron diffraction and magnetization measurements. In agreement with the previously published results, the low-temperature zero-field structure is characterized by two half-integer propagation vectors $\mathbf{k}_1 = [\frac{1}{2}\,0\,\frac{1}{2}]$ and $\mathbf{k}_2 = [\frac{1}{2}\,\frac{1}{2}\,\frac{1}{2}]$. However, on application of an external magnetic field, the Bragg peaks corresponding to the zero-field structure lose their intensity rather rapidly and disappear completely in a field of 2.5 kOe. In the intermediate fields, 2.5 to 22.5 kOe, new peaks are observed characterized by the propagation vector $\mathbf{k}' = [0\,0\,\frac{1}{3}]$ corresponding to an *up-up-down* (uud) structure as well $\mathbf{k} = 0$ ferromagnetic peaks. This regime of fields corresponds to a pronounced plateau in the magnetization curve. Remarkably, the uud structure survives heating to at least 1.4 K, three times higher temperature than the T_N of 0.48 K for the zero-field structure. Above 22.5 kOe, the $\mathbf{k}'$ peaks disappear while the $\mathbf{k} = 0$ peaks gain significant intensity indicating an increase in the polarization of the system. The analysis of the intensities of the field-induced reflections allows for a clear identification of the magnetic structures in both the intermediate- and high-field regimes.

I. INTRODUCTION

Binary rare-earth (RE) oxides ARE$_2$O$_4$, where A is Ba, Ca, Sr, or Eu, have been actively studied for their potential in various applications, particularly in optics and photoluminescence [1–5]. The high density of the materials and large magnetic moments associated with the RE ions also make them promising for low-temperature demagnetization cooling applications, as magnetocaloric effects are significant [6,7]. Interest in the fundamental magnetic properties of the ARE$_2$O$_4$ oxides was ignited by the realization that the magnetic RE ions form zigzag ladders and therefore are likely to be governed by geometrically frustrated interactions [8]. Further studies of several members of the family have confirmed this conjecture and reported the behavior typically associated with frustrated magnetism, i.e., reduced transition temperatures, partial magnetic ordering, coexistence of different magnetic structures, as well as a high sensitivity to an applied field [9–13].

One of the family members, BaDy$_2$O$_4$, has recently been reported to order magnetically below $T_N = 0.48$ K [14] with the ground state being characterized by the two propagation vectors $\mathbf{k}_1 = [\frac{1}{2}\,0\,\frac{1}{2}]$ and $\mathbf{k}_2 = [\frac{1}{2}\,\frac{1}{2}\,\frac{1}{2}]$. This behavior is in sharp contrast to the properties of SrDy$_2$O$_4$, a homologous compound with very similar unit-cell parameters as well as the positions of the magnetic Dy^{3+} ions within the unit cell [8,14,15] (see Fig. 1). In zero field, SrDy$_2$O$_4$ lacks three-dimensional long-range magnetic order down to temperatures as low as 60 mK, its zero-field magnetic structure consists of a collection of antiferromagnetic chains running along the c axis with very little correlations between the chains [16]. It has been argued that one-dimensional trapped domain walls

are responsible for the suppression of the three-dimensional (3D) order in zero field in this compound [17]. However, an *up-up-down* (uud) state with much longer correlations can be induced in SrDy$_2$O$_4$ by a magnetic field applied along the b axis [16]. The field-induced magnetic ordering in SrDy$_2$O$_4$ for $H \parallel b$ is best seen in single-crystal calorimetry [18], ultrasound [19], and neutron diffraction [16,20] measurements, although, even in a polycrystalline neutron diffraction experiment [16], the powder-averaged signal is dominated by the sharp magnetic Bragg peaks formed on top of broad diffuse features seen in zero field. The uud states are characterized by a $\frac{1}{3}$-magnetization plateau and have also been observed in other compounds in the SrRE$_2$O$_4$ family, such as SrEr$_2$O$_4$ and SrHo$_2$O$_4$ [21].

Unlike the case of SrDy$_2$O$_4$ for which large single-crystal samples have been available for some time [22], BaDy$_2$O$_4$ has so far only been synthesized in a polycrystalline form or as crystals not exceeding $1.0 \times 0.1 \times 0.1$ mm^3 in size [23], therefore, detailed single-crystal neutron diffraction studies of BaDy$_2$O$_4$ remain problematic. In this paper we report the low-temperature in-field behavior of BaDy$_2$O$_4$ investigated through powder neutron diffraction (PND) experiments as well as magnetization measurements. We followed the evolution of the magnetic structure with an applied magnetic field and found that in the intermediate fields, 2.5 to 22.5 kOe, an antiferromagnetic field-induced order is markedly different from the zero-field structure, while the fields above 30 kOe stabilize a polarized $\mathbf{k} = 0$ state, where only one of the Dy^{3+} sites has magnetic moments pointing predominantly along the b axis while the other site remains largely disordered. Remarkably, the antiferromagnetic field-induced structure characterized by the propagation vector $(00\frac{1}{3})$
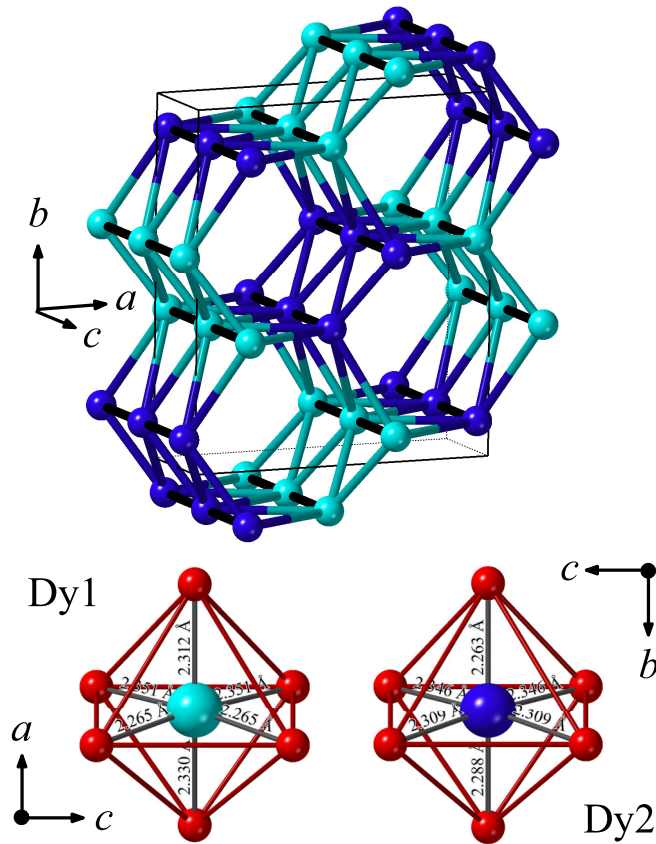
FIG. 1. (Top) Positions of the magnetic Dy^{3+} ions within $BaDy_2O_4$. The Dy1 and Dy2 crystallographic positions (space group *Pnam*) are shown in different colours. (Bottom) DyO_6 octahedra for the Dy^{3+} ions in the two crystallographic position, Dy1 (left) and Dy2 (right), with the distances to the nearest oxygen atoms labeled [22].

appears to be much more robust than the zero-field state, as it survives to temperatures as high as three times $T_N(H = 0)$.

II. EXPERIMENTAL PROCEDURES

Polycrystalline samples of $BaDy_2O_4$ were prepared by the conventional solid-state synthesis method following previous reports on preparing this material [14,15,22]. High purity Dy_2O_3 (99.99%) and $BaCO_3$ (99.98%) were used as starting materials. To ensure the appropriate composition of the final compound, the dysprosium oxide was preannealed in air at $1000\,°C$ overnight. A 12.5% excess of $BaCO_3$ was added to compensate for the loss of barium due to evaporation during the synthesis process. Powders of the starting materials were weighed, mixed together, and pressed into pellets to facilitate the chemical reaction. The pellets were then transferred into an alumina boat and heated at $1200\,°C$–$1300\,°C$ in flowing $Ar+3\%H_2$ gas atmosphere for 4-8 h [15]. Powder x-ray diffraction measurements, using a Panalytical x-ray diffractometer with a Cu $K\alpha 1$ anode ($\lambda = 1.5406$ Å), were used to check the composition of the $BaDy_2O_4$ sample prior to the neutron diffraction measurements.

The magnetization measurements were made in applied magnetic fields of up to 70 kOe using a Quantum Design MPMS SQuID magnetometer. An iQuantum ^{3}He insert [24] allowed the temperature range explored to be extended down to 0.48 K.

PND experiments were conducted on the WISH time-of-flight diffractometer [25] at the ISIS facility at the Rutherford Appleton Laboratory (STFC, UK) in a range of temperatures from 40 mK to 10 K and in fields of up to 60 kOe. A dilution refrigerator inside a vertical-field cryomagnet (with the opening of $\pm 7.5°$) provided the necessary sample environment. The sample was placed inside an annular-shaped thin-wall copper container in order to minimize high neutron absorption caused mainly by ^{161}Dy and ^{164}Dy isotopes in naturally occurring dysprosium. We were able to add extra He exchange gas to the container during the measurements to ensure full thermal stabilization of the sample. This feature of the experimental setup has proved to be crucial in reaching low temperatures for a sample with very limited thermal conductivity.

We used the data obtained in zero field at $T = 10$ K as a background to isolate the magnetic signal. On application of an external magnetic field, a significant redistribution of the grains in the powder sample was observed, as the data taken in a zero field afterwards demonstrate the presence of preferred orientation effects. This unavoidable complication has resulted in a small "oversubtraction" for the background signal for some fields and restricted the accuracy of the magnetic Bragg peak's intensity integration.

III. RESULTS AND DISCUSSION

A. Magnetization measurements

For $T > 2$ K, the temperature dependence of magnetic susceptibility, $\chi(T)$, in $BaDy_2O_4$ (see Fig. 2) demonstrates a behavior consistent with the previous observations [15,22]. Although never perfectly linear, the $\chi^{-1}(T)$ largely follows the Curie-Weiss law for $T > 20$ K. When restricted to the temperature range 45 to 300 K, a linear fit to $\chi^{-1}(T)$ returns the Weiss temperature Θ of $-7.1(1)$ K and the effective magnetic moment μ_{eff} on the Dy^{3+} ions of $10.36(1)\mu_B$. While the observed magnetic moment is very close to the value calculated using Hund's rules as well as the reported values, Θ is significantly smaller (in absolute value) compared to -23.5 K from Ref. [15] and to $-11.5(4)$ K from Ref. [22]. The difference is most likely due to the different temperature ranges used for the fitting, as well as the presence of ferromagnetic impurities (up to a 2% level) in the samples prepared using stainless steel crucibles, as in Ref. [22].

On extending the temperature range for the measurements down to 0.48 K (see the inset in Fig. 2) we find that the susceptibility continues to grow at lower temperature until about 0.6 K, where it exhibits a broad maximum before reducing slightly at lower T. The observed broad maximum in $\chi(T)$ is likely to be a precursor for the ordering transition expected at 0.48 K [14] with the transition temperature itself being marked by a very sharp decrease in $\chi(T)$, as has been seen in powder samples of $BaNd_2O_4$ [12] and $SrNd_2O_4$ [26].
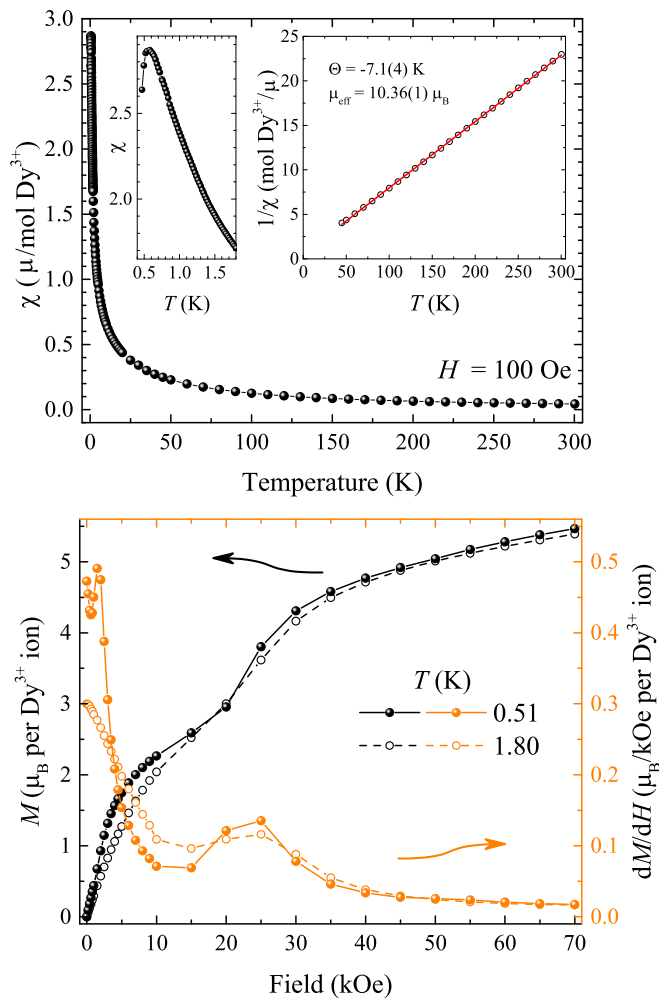
FIG. 2. (Top) Temperature dependence of the magnetic susceptibility of $BaDy_2O_4$ measured in a field of 100 Oe. The left inset expands on the low-temperature part of the data, the right inset shows a linear fit to the inverse susceptibility performed in the range 45 to 300 K. (Bottom) Magnetization $M(H)$ and its derivative dM/dH measured at two different temperatures, 0.51 and 1.80 K.

Magnetization versus field $M(H)$ curves have been measured at 0.51 and 1.80 K. At both temperatures there is a plateau (that is more pronounced at lower T) from about 5 to 20 kOe (see Fig. 2). The magnetic moment grows continuously in higher fields reaching $5.5\mu_B$ per Dy^{3+} ion in 70 kOe, suggesting that in this field the system is far from full saturation. The value of magnetization on the plateau, around $2.4\mu_B$, amounts to significantly more than a third of the magnetization measured in 70 kOe, however, this result for a powder-averaged measurement on a sample containing two magnetic sites is not surprising. In fact, the existence of the magnetization plateaus is a common feature for many $SrRE_2O_4$ compounds, but their presence is much more obvious in the $M(H)$ curves of single crystals [21] rather than powder samples [8]. However, even for powder samples the derivative of the magnetization dM/dH demonstrates a clear minimum associated with a plateau and in that respect the magnetization data for $BaDy_2O_4$ (see Fig. 2) look remarkably similar to what has been reported for $SrDy_2O_4$ [8].
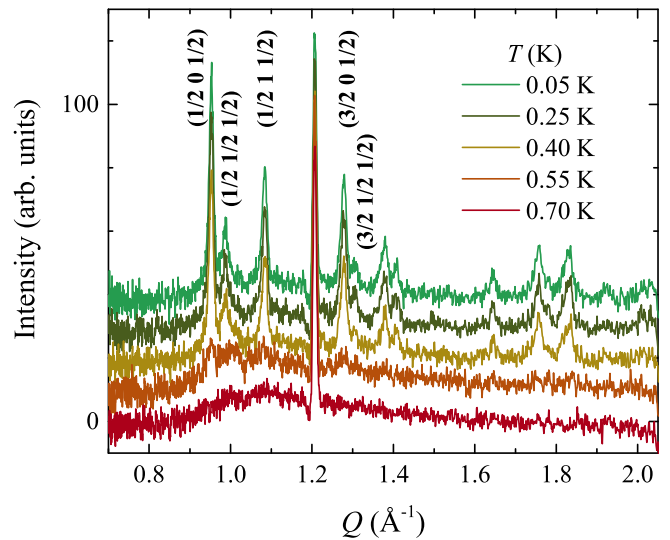

FIG. 3. Temperature evolution of the magnetic neutron diffraction patterns of $BaDy_2O_4$ in zero applied field. The magnetic contribution is obtained by subtracting a 10-K background. The sharp feature at $1.206\,\text{Å}^{-1}$ is an artifact due to redistribution of the grains in the powder sample in an applied field (see text).

B. Powder neutron diffraction

In zero field, powder neutron diffraction measurements on $BaDy_2O_4$ reveal the presence of strong diffuse background signal at higher temperatures and the development of magnetic Bragg peaks at low temperatures, as shown in Fig. 3. In good agreement with the previously published data [14], the peaks are largely confined to temperatures below 0.5 K, as for $T = 0.55$ K only remnants of the strongest reflections are present. The peaks can be indexed using two propagation vectors $\mathbf{k}_1 = [\frac{1}{2}0\frac{1}{2}]$ and $\mathbf{k}_2 = [\frac{1}{2}\frac{1}{2}\frac{1}{2}]$, the indices are given in Fig. 3 for the first five peaks observed at the lowest Q. Note that the zero-field data at higher temperatures were collected after the sample's exposure to high fields at the base temperature. Therefore, in Fig. 3 there is a large nuclear peak at $1.206\,\text{Å}^{-1}$, which appears due to a preferred alignment of the powder grains by the applied field. As the zero-field magnetic structure has been discussed in Ref. [14] we do not discuss it in any detail in this paper, focusing instead on the in-field behavior.

Figure 4 shows the development of the magnetic diffraction patterns of $BaDy_2O_4$ with the applied magnetic field at the base temperature of the cryomagnet, 0.05 K. We used a 10-K background to isolate the magnetic contribution presuming that the nuclear intensity from the $BaDy_2O_4$ as well as (predominantly copper) intensity from the sample environment remains temperature independent below 10 K. Although the magnetic signal was seen in all 10 detector banks on the WISH diffractometer, we focus mostly on the diffraction patterns from pairs of banks, 2 and 9, and, 3 and 8 as they provide good Q-range coverage combined with high flux and resolution.

The first clear observation from Fig. 4 is that the zero-field antiferromagnetic peaks, the strongest being observed at 0.953 and $1.084\,\text{Å}^{-1}$, start losing their intensity very quickly in an applied field (they are only a half as strong in 1.25 kOe
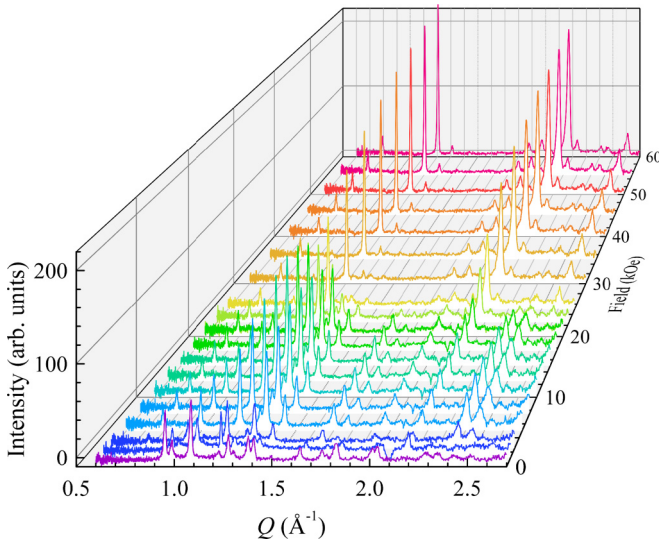
FIG. 4. Evolution of the magnetic neutron diffraction patterns of $BaDy_2O_4$ with an applied field at $T = 0.05$ K in the range 0 to 60 kOe as measured by detector banks 2 and 9 of the WISH diffractometer. The magnetic contribution is obtained by subtracting a 10-K background.

FIG. 5. Field dependence of the intensity for the (top panel) AFM and (bottom panel) FM peaks in $BaDy_2O_4$. The peaks are labeled by their scattering vector positions. The intensity of the peaks at 2.234 and 2.609 Å is increased by a factor of 5. The intensity is obtained by integrating the peaks above zero after subtracting a 10-K background signal.

compared to zero field) and by 2.5 kOe they completely disappear. Within the accuracy of our measurements, the applied magnetic field affects to the same extent the zero-field peaks described by the two propagation vectors $\mathbf{k}_1$ and $\mathbf{k}_2$, although much more detailed measurements would be required to make a definitive statement. This extreme sensitivity of the ground state to a weak perturbation is unusual, but not entirely unexpected: in zero field, the magnetic structure, which appears below 0.48 K, seems to have Bragg peaks *not* in the positions where diffuse signal is the strongest at $T > T_N$, as best seen in the two-dimensional color plots [Fig. 6(a) of Ref. [14]]. It is therefore reasonable to surmise that in zero field, there are several nearly degenerate states which $BaDy_2O_4$ could adopt and that the ground state has an energy marginally lower than the states influencing the short-range correlations just above the T_N. Given this peculiar behavior, it might be of interest to revisit the zero-field diffraction data obtained above the ordering temperature and to employ reverse Monte Carlo refinements to study the magnetic correlations [27,28].

Instead of the zero-field peaks, the applied field induces two other sets of magnetic Bragg peaks. The intensities of the first set of reflections appear in the intermediate applied fields and then vanish rather rapidly in higher applied fields, becoming negligibly small in fields above 25 kOe, we label these peaks as antiferromagnetic (AFM). Another set of peaks gain some intensity in intermediate fields, continue to increase in intensity in higher fields, show a tendency to saturation, but do not fully saturate in the highest applied field of 60 kOe. We label these peaks as ferromagnetic (FM). This drastically different behavior of the two sets of peaks is emphasized in Fig. 5 which shows the field dependence of the intensity of a selected number of the AFM and FM peaks. Figure 5 also provides a natural way to introduce more accurately the definitions of the intermediate- and high-field regions, the former being from 2.5 to 25 kOe and the latter above 25 kOe.
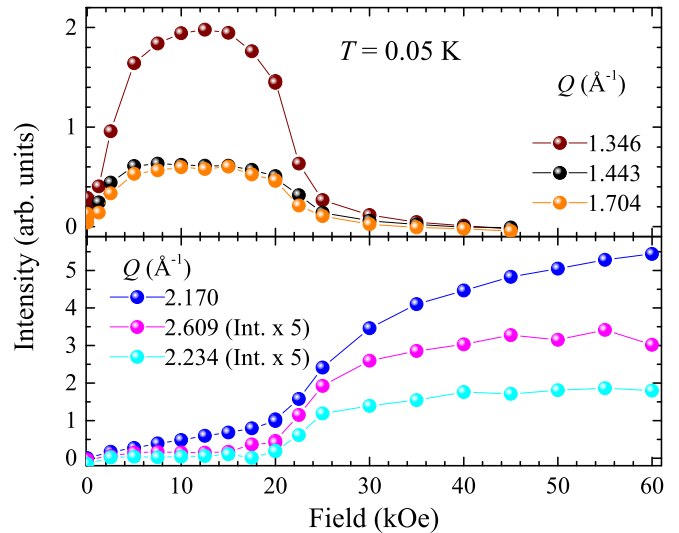
The intermediate-field region coincides with the stabilization of a magnetization plateau. The hysteretic effects seem to be less pronounced in $BaDy_2O_4$ compared to $SrDy_2O_4$[19,20] and $SrEr_2O_4$ [29], as the zero-field ground state is restored when the applied field is ramped back down to zero after field excursions to 20 and 60 kOe.

Despite the natural limitations of magnetic structure determination from PND in an applied magnetic field, we were able to refine the diffraction data both in the FM (60 kOe) and the AFM (12.5 kOe) regimes (see Fig. 6). The high-field data (60 kOe) can be successfully fitted assuming a simple ferromagnetic ordering with the moments aligned along the b axis. The refinement yields the ordering only on one Dy site with the ordered moment of $9.44(5)\mu_B$, and no statistically significant ordered component along the a, b, or c directions was detected for the second Dy site. Attempts to constrain the moment size of Dy1 and Dy2 to be equal failed to reproduce the experimental diffraction pattern. It is impossible to determine from the powder diffraction data which of the Dy^{3+} ions on crystallographically inequivalent sites participate in the formation of the FM state and which stays disordered, as both possibilities provide equally good fits to the data. However, the crystalline electric field calculations reported in Ref. [14] indicate that the Dy1 and Dy2 sites have the easy axes parallel to the a and b directions, respectively. The Dy2 site also has a very large separation between the ground state and the first excited doublet [14] and therefore is likely to possess an almost perfect Ising-like magnetic moment. This observation provides a good reason to locate the ordered moment of the high-field phase of $BaDy_2O_4$ on the Dy2 site, as shown in Fig. 7(a).

Apparently, the presence of only one ordered site is closely related to the substantial preferred orientation of the powder particles induced by the applied magnetic field. The
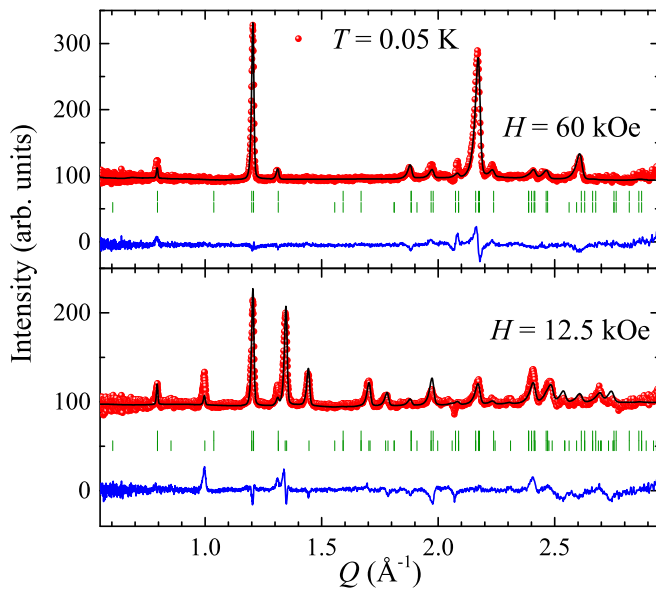
FIG. 6. Rietveld refinement of the PND data in an applied magnetic field of (top panel) 60 kOe and (bottom panel) 12.5 kOe at 0.05 K. The experimental data (red circles) from banks 2 and 9 of the WISH diffractometer [25] after subtracting a 10-K background signal, calculated patterns (black lines) and the difference curves (blue lines) are shown. Ticks represent the positions of the nuclear and magnetic Bragg peaks.

refinement reveals that a significant fraction of the sample is textured with the preferred orientation vector (0,1,0) lying along the direction of the applied field. Removing the applied field does not recover the initial statistically random distribution of the powder grains, therefore, the intensities of some of the nuclear and magnetic peaks are affected by exposure to the magnetic field.

A similar situation, where only one site is ordered and the sample is substantially textured, has been found in the intermediate-field regime, 2.5 to 25 kOe. For this field region the magnetic peaks are indexed with two propagation
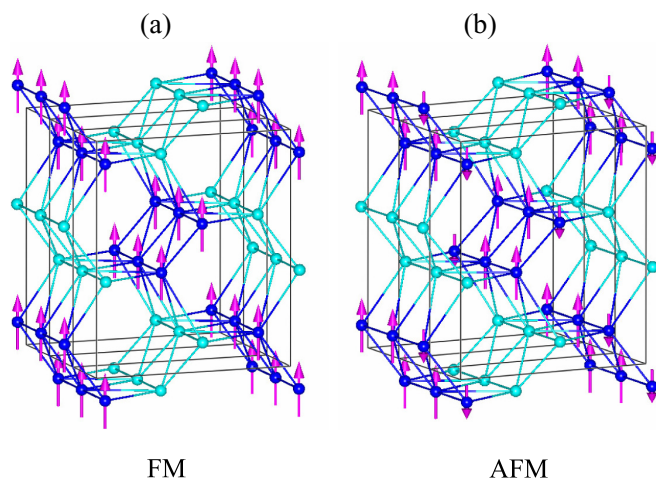

FIG. 7. Magnetic structures of $BaDy_2O_4$ in the (a) FM and (b) AFM regimes as obtained from PND data refinements at $T = 0.05$ K.
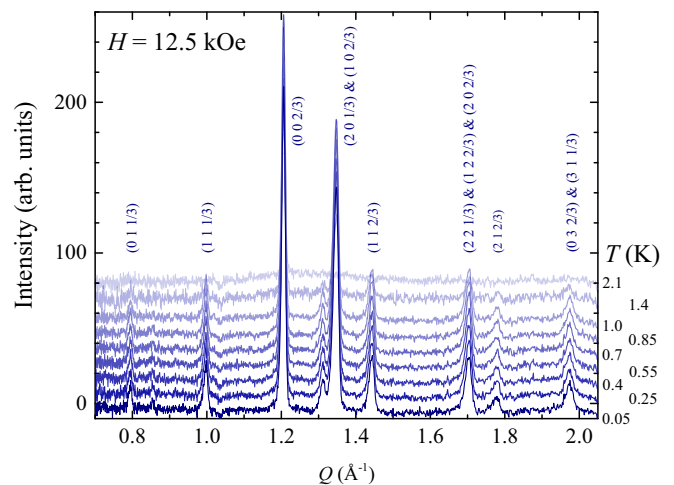

FIG. 8. Temperature evolution of the magnetic diffraction patterns of $BaDy_2O_4$ in 12.5 kOe. The magnetic contribution is obtained but subtracting the 10-K zero-field background. The curves are consecutively offset by 10 units for clarity.

vectors $\mathbf{k} = 0$ and $\mathbf{k}' = [0\,0\,\frac{1}{3}]$. These coexisting propagation vectors strongly point to the uud type of the magnetic structure. Indeed, the model where magnetic phases of the four symmetry-related Dy sites in the $4c$ Wyckoff position differ by $\frac{2\pi}{3}$ provides a reasonably good quality fit for the experimentally observed intensities (Fig. 6). The corresponding uud magnetic structure with moments polarized along the b axis is shown in Fig. 7(b). The ordered moments for the up and down spins are $9.2(1)\mu_B$ and $5.8(1)\mu_B$, respectively, refined for the diffraction pattern collected at 12.5 kOe. Again, it was not possible to decide which Dy1 or Dy2 carries the ordered moments based on the refinement quality, but the moment direction strongly suggests the Dy2 site.

Figure 8 shows the evolution of the diffraction patterns observed in an intermediate field of 12.5 kOe with increasing temperature. It is rather clear that none of the AFM peaks are greatly affected by the temperature increase until well above $T_N(H = 0)$. In fact, they show almost no temperature dependence for temperatures below 1 K, survive at temperature as high as 1.4 K, and disappear completely only at $T = 2.1$ K. We have also collected diffraction data in a field of 5 kOe (not shown) in increasing temperature, which support the observation that the AFM phase survives at temperature above 1.4 K. Note, the rather sparse temperature points at higher temperatures is due to the limitations imposed by the dilution refrigerator used, as it cannot maintain temperatures above 1 K for time sufficiently long to collect data, while the base temperature of the cryomagnet without dilution refrigerator cooling was 2.1 K.

As stated above, the appearance of the magnetization plateaus is a common feature of many similar $SrRE_2O_4$ compounds [21,30]. What makes the $BaDy_2O_4$ case unusual is the fact that the field-induced uud state in this compound seems to be completely different from the zero-field structure rather than evolving from it. In $SrHo_2O_4$, for example [31], the main effect of a field applied along the b axis is in the evolution of the diffuse magnetic scattering to a set of nearly

resolution-limited Bragg peaks associated with the uud state. Similarly in $SrEr_2O_4$, a field applied parallel to the *a* axis drives the planes of diffuse scattering observed in zero field to much more localized, but still diffuse, features, corresponding to the establishment of the uud structure and the associated $\frac{1}{3}$-magnetization plateau [29]. In the absence of single-crystal samples of $BaDy_2O_4$ large enough for neutron diffraction, however, it will be extremely difficult to check if in this compound the field-induced uud state also has a diffuse precursor in zero field.

The axial next-nearest-neighbor Ising (ANNNI) model [32,33] has been employed to describe the magnetic properties of $SrHo_2O_4$ [13], $SrDy_2O_4$ [17,20], and other members of the family. Although the model captures several features (including the uud state for longitudinal fields) and allows for the introduction of the effective exchange constants, it is as a minimal effective model in which the interactions between the ladders are ignored. An exact, albeit incomplete, solution of the ground-state problem for an Ising model on a 3D honeycomb zigzag ladder lattice with two types of sites has recently been proposed using the method of basic sets of cluster configurations [34]. This approach shows that frustration leads to the appearance of a large variety of magnetic phases, most of them being partially disordered and that the sequence of field-induced transitions in the honeycomb zigzag ladder magnets could potentially be even more complicated with the appearance of several "intermediate" phases separating the zero field, the uud, and the field-polarized states.

Given an unusual robustness of the field-induced AFM state it might also be of interest to perform further magnetocaloric effect measurements on $BaDy_2O_4$ with a view to using it as a cryogenic refrigerant material [6,7].

IV. CONCLUSIONS

In conclusion, we have investigated the in-field behavior of $BaDy_2O_4$ at low temperatures and found that the zero-field state is very sensitive to the external fields as it is removed by the application of 2.5 kOe. We also find that in this zigzag ladder compound an uud structure, corresponding to a magnetization plateau is induced by the fields between 2.5 and 25 kO, while a polarized FM state is supported in fields above 25 kOe. Remarkably, the field-induced uud structure is much more stable in higher temperatures compared to the zero-field state, as it survives warming to the three times higher temperature than the $T_N(H = 0)$. We hope that this experimental discovery will stimulate further theoretical developments for the ground-state selection in frustrated systems, particularly in an applied field.

[1] X.-Y. Sun, W.-F. Wang, S.-Q. Sun, L.-W. Lin, D.-Y. Li, and L.-P. Zhou, Luminescence **28**, 384 (2013).

[2] J. Singh and J. Manam, Ceram. Int. **42**, 18536 (2016).

[3] K.-H. Kim, E.-H. Kang, B.-K. Kang, K. P. Kim, and S.-H. Hong, J. Lumin. **183**, 13 (2017).

[4] D. Taikar, J. Lumin. **204**, 24 (2018).

[5] S. Zhang, Z. Hao, L. Zhang, G.-H. Pan, H. Wu, H. Wu, Y. Luo, X. Liu, H. Zhang, and J. Zhang, Dalton Trans. **48**, 5263 (2019).

[6] A. Midya, N. Khan, D. Bhoi, and P. Mandal, Appl. Phys. Lett. **101**, 132415 (2012).

[7] X. Jiang, Z. W. Ouyang, Z. X. Wang, Z. C. Xia, and G. H. Rao, J. Phys. D: Appl. Phys. **51**, 045001 (2018).

[8] H. Karunadasa, Q. Huang, B. G. Ueland, J. W. Lynn, P. Schiffer, K. A. Regan, and R. J. Cava, Phys. Rev. B **71**, 144414 (2005).

[9] O. A. Petrenko, G. Balakrishnan, N. R. Wilson, S. de Brion, E. Suard, and L. C. Chapon, Phys. Rev. B **78**, 184410 (2008).

[10] D. L. Quintero-Castro, B. Lake, M. Reehuis, A. Niazi, H. Ryll, A. T. M. N. Islam, T. Fennell, S. A. J. Kimber, B. Klemke, J. Ollivier, V. G. Sakai, P. P. Deen, and H. Mutka, Phys. Rev. B **86**, 064203 (2012).

[11] O. Young, A. R. Wildes, P. Manuel, B. Ouladdiaf, D. D. Khalyavin, G. Balakrishnan, and O. A. Petrenko, Phys. Rev. B **88**, 024411 (2013).

[12] A. A. Aczel, L. Li, V. O. Garlea, J.-Q. Yan, F. Weickert, M. Jaime, B. Maiorov, R. Movshovich, L. Civale, V. Keppens, and D. Mandrus, Phys. Rev. B **90**, 134403 (2014).

[13] J.-J. Wen, W. Tian, V. O. Garlea, S. M. Koohpayeh, T. M. McQueen, H.-F. Li, J.-Q. Yan, J. A. Rodriguez-Rivera, D. Vaknin, and C. L. Broholm, Phys. Rev. B **91**, 054424 (2015).

[14] B. Prévost, N. Gauthier, V. Y. Pomjakushin, B. Delley, H. C. Walker, M. Kenzelmann, and A. D. Bianchi, Phys. Rev. B **98**, 144428 (2018).

[15] Y. Doi, W. Nakamori, and Y. Hinatsu, J. Phys.: Condens. Matter **18**, 333 (2006).

[16] O. A. Petrenko, O. Young, D. Brunt, G. Balakrishnan, P. Manuel, D. D. Khalyavin, and C. Ritter, Phys. Rev. B **95**, 104442 (2017).

[17] N. Gauthier, A. Fennell, B. Prévost, A.-C. Uldry, B. Delley, R. Sibille, A. Désilets-Benoit, H. A. Dabkowska, G. J. Nilsen, L.-P. Regnault, J. S. White, C. Niedermayer, V. Pomjakushin, A. D. Bianchi, and M. Kenzelmann, Phys. Rev. B **95**, 134430 (2017).

[18] T. H. Cheffings, M. R. Lees, G. Balakrishnan, and O. A. Petrenko, J. Phys.: Condens. Matter **25**, 256001 (2013).

[19] C. Bidaud, O. Simard, G. Quirion, B. Prévost, S. Daneau, A. D. Bianchi, H. A. Dabkowska, and J. A. Quilliam, Phys. Rev. B **93**, 060404(R) (2016).

[20] N. Gauthier, A. Fennell, B. Prévost, A. Désilets-Benoit, H. A. Dabkowska, O. Zaharko, M. Frontzek, R. Sibille, A. D. Bianchi, and M. Kenzelmann, Phys. Rev. B **95**, 184436 (2017).

[21] T. J. Hayes, O. Young, G. Balakrishnan, and O. A. Petrenko, J. Phys. Soc. Jpn. **81**, 024708 (2012).

[22] G. Balakrishnan, T. J. Hayes, O. A. Petrenko, and D. McK Paul, J. Phys.: Condens. Matter **21**, 012202 (2009).

[23] T. Besara, M. S. Lundberg, J. Sun, D. Ramirez, L. Dong, J. B. Whalen, R. Vasquez, F. Herrera, J. R. Allen, M. W. Davidson, and T. Siegrist, Prog. Solid State Chem. **42**, 23 (2014).

[24] N. Shirakawa, H. Horinouchi, and Y. Yoshida, J. Magn. Magn. Mater. **272-276**, E149 (2004).

[25] L. C. Chapon, P. Manuel, P. G. Radaelli, C. Benson, L. Perrott, S. Ansell, N. Rhodes, D. Raspino, D. Duxbury, E. Spill, and J. Norris, Neutron News **22**, 22 (2011).

[26] N. Qureshi, A. Wildes, C. Ritter, B. Fåk, S. X. M. Riberolles, M. Ciomaga Hatnean, and O. A. Petrenko, Phys. Rev. B **103**, 134433 (2021).

[27] J. A. M. Paddison and A. L. Goodwin, Phys. Rev. Lett. **108**, 017204 (2012).

[28] J. A. M. Paddison, J. R. Stewart, and A. L. Goodwin, J. Phys.: Condens. Matter **25**, 454220 (2013).

[29] N. Qureshi, O. Fabelo, P. Manuel, D. D. Khalyavin, E. Lhotel, S. Riberolles, G. Balakrishnan, and O. A. Petrenko (unpublished).

[30] O. A. Petrenko, Low Temp. Phys. **40**, 106 (2014).

[31] O. Young, G. Balakrishnan, P. Manuel, D. D. Khalyavin, A. R. Wildes, and O. A. Petrenko, Crystals **9**, 488 (2019).

[32] T. Morita and T. Horiguchi, Phys. Lett. A **38**, 223 (1972).

[33] W. Selke, Phys. Rep. **170**, 213 (1988).

[34] Y. I. Dublenych and O. A. Petrenko, An Ising model on a 3D honeycomb zigzag-ladder lattice: A solution to the ground-state problem and application to the $SrRE_2O_4$ and $BaRE_2O_4$ magnets, arXiv:2008.06445.